

and then $\bar{p}(S) = 1$. Now suppose that $\bar{p}(S) \geq p > 1$ and that the boundary values of G_{p-1} are infinite. From (12) a boundary value of G_p can be finite only if $|\hat{\beta}_p| = 1$, then from (11) we obtain

$$\hat{\epsilon}_r(t; p) = \sum_{k=0}^p \hat{a}_k x_r(t-k) = 0,$$

$$t = p+1, \dots, m, \quad r = 1, \dots, n$$

and $\bar{p}(S) = p$.

Finally, we must show that for $p \geq p(S)$ the MLE does not exist. It is sufficient to take $p = p(S)$. Let $(\hat{\beta}_1, \dots, \hat{\beta}_p)$ be a set of reflection coefficients with $|\hat{\beta}_k| < 1$ for $k < p$ and $|\hat{\beta}_p| = 1$ leading through (5) to the condition (6) in the definition of $p(S)$. From the expression (10) of G_p we obtain, for β_p in a neighbourhood of $\hat{\beta}_p$,

$$G_p(\hat{\beta}_1, \dots, \hat{\beta}_{p-1}, \beta_p; S) \sim C[1 - |\beta_p|^2]^{(m-p)/m}$$

where C stands for some constant, so G_p tends to zero in this boundary point.

V. CONCLUSION

We have proved that for almost all sets of n records of length m of complex data, the MLE in AR (p) models exists if and only if the n records can not be exactly fitted by complex undamped sinusoids using the same set of p distinct frequencies. So in estimating AR (p) models with increasing order p , the maximum likelihood method can be applied until $p = m - 1$ or stops with p just smaller than the minimal number of frequencies $p(S)$ used by the sinusoids fitting the data exactly. The method in [4] working on the reflection coefficients, its use with $p = p(S)$ gives, in the limit, the borderline values $\hat{\beta}_1, \dots, \hat{\beta}_{p(S)}$ with $|\hat{\beta}_{p(S)}| = 1$ describing the average of the discrete spectrum of these sinusoids.

REFERENCES

- [1] T. E. Barnard, "Two maximum beamforming algorithms for equally spaced line arrays," *IEEE Trans. Acoust., Speech, Signal Processing*, vol. ASSP-30, pp. 175-189, Apr. 1982.
- [2] D. T. Pham and S. Degerine, "Efficient computation of autoregressive estimates through a sufficient statistics," *IEEE Trans. Acoust., Speech, Signal Processing*, vol. 38, pp. 1693-1698, Jan. 1990.
- [3] D. T. Pham, "Maximum likelihood estimation of autoregressive model by relaxation on the reflection coefficients," *IEEE Trans. Acoust., Speech, Signal Processing*, vol. ASSP-36, pp. 1363-1367, Aug. 1988.
- [4] D. T. Pham, A. Le Breton, and D. Q. Tong, "Maximum likelihood estimation for complex autoregressive model and Toeplitz interspectral matrices," in *Signal Processing IV, Proc. 4th EUSIPCO* (Grenoble, France, vol. 1, 1988, pp. 47-50).
- [5] S. Degerine, "On local maxima of the likelihood function for Toeplitz matrix estimation," *IEEE Trans. Signal Processing*, vol. 40, no. 6, pp. 1563-1565, June 1992.
- [6] S. Degerine, "Maximum likelihood estimation of autocovariance matrices from replicated short time series," *J. Time Series Anal.*, vol. 8, pp. 135-146, 1987.
- [7] M. I. Miller and D. L. Snyder, "The role of likelihood and entropy in incomplete-data problems: Applications to estimating point process intensities and Toeplitz constrained covariances," *Proc. IEEE*, vol. 75, no. 7, pp. 892-907, 1987.
- [8] S. Degerine, "Comportement au bord et caractérisation d'un maximum pour la vraisemblance d'un vecteur aléatoire gaussien centré avec contrainte sur sa structure de covariance," *C. R. Acad. Sci. (this is Paris)*, t. 301, série I, no. 5, pp. 233-236, 1985.

Estimation of Multiple Sinusoidal Frequencies Using Truncated Least Squares Methods

S. F. Hsieh, K. J. R. Liu, and K. Yao

Abstract—Various SVD-based methods have been shown effective for resolving closely spaced frequencies. However, the massive computations required by SVD makes it unsuitable for real-time applications. To reduce the computational complexity, three truncated QR methods are proposed: 1) truncated QR without column pivoting (TQR); 2) truncated QR with reordered columns (TQRR); and 3) truncated QR with column pivoting (TQRP). It is demonstrated that many of the benefits of the SVD-based methods are achievable under the truncated QR methods with much lower computational cost. Based on the forward-backward linear prediction model, computer simulations and comparisons are provided for different truncation methods under various SNR's. Comparisons of asymptotic performance with large data samples are also given.

I. INTRODUCTION

In the pioneering paper of Tufts and Kumaresan [3], a SVD-based method for solving the forward-backward linear prediction (FBLP) least squares (LS) problem was used to resolve the frequencies of closely spaced sinusoids from a limited amount of data samples. By imposing an excessive order in the FBLP model and then truncating small singular values to zero, this truncated SVD (TSVD) method yields a low SNR threshold and greatly suppresses spurious frequencies. However, the massive computations required by SVD makes it unsuitable for real-time superresolution applications. We propose using truncated QR and LS methods which are more amenable to VLSI implementations, such as on systolic arrays [8], with insignificantly degraded performances as compared to the TSVD method. Three different truncated QR methods are considered, depending on the ordering of the columns of the data matrix. The first one is the truncated QR method without column shuffling (TQR). This method does not change the structure of the data matrix. A QR decomposition (QRD) of the data matrix is followed by the truncation of the lower right weak-rank submatrix of the upper-triangular matrix. The second one is the truncated QR method with reordered columns (TQRR). The reordering of the columns is determined in an *a priori* manner [6]. Here truncation is performed on the QRD of the column-reordered data matrix. The computational cost of this TQRR method is the same as that of the first method, except for the column reshuffling. The last one is called truncated QR with column pivoting (TQRP) [9]. This method entails a series of dynamic swapping of columns while performing the QRD. An additional computational cost is required to monitor the norms of the remaining columns in the dimension-shrinking

Manuscript received August 6, 1990; revised December 31, 1991. This work was supported in part by the National Science Council of the Republic of China under Grant NSC80-E-SP-009-01A, the NSF Engineering Center Grant ECD-8803012, the NASA/Ames Grant NCR-8814407, and a UC MICRO Grant. An earlier version of the paper was presented at the 2nd International Workshop on SVD and Signal Processing and published in the workshop proceedings *SVD and Signal Processing II*, R. J. Vaccaro, Ed., Elsevier Science Publishers, 1991.

S. F. Hsieh is with the Department of Communication Engineering, National Chiao Tung University, Hsinchu, Taiwan, Republic of China 30039.

K. J. R. Liu is with the Department of Electrical Engineering, Systems Research Center, University of Maryland, College Park, MD 20742.

K. Yao is with the Department of Electrical Engineering, University of California, Los Angeles, CA 90024-1594.

IEEE Log Number 9205123.

submatrix such that the first column is replaced by the one with the largest norm in the remaining submatrix. The processing overhead of successive column swapping may be nontrivial and prohibitive in implementing a VLSI structure. All these three truncated QR methods only involve a finite number of computations, while for the TSVD method, it is well known that the number of iterations required cannot be specified exactly. Based upon Matlab computations, SVD requires about 5 to 6 times the number of flops compared to the QRD for a dense 50×50 matrix. Furthermore, we should note that the QRD only requires a small number of flops for updating when new data are successively appended [8], [9]. Exact updating of the SVD is generally much more intractable [10], although efficient updating techniques do exist at the expense of decreased accuracy [11].

A FBLP model for estimating sinusoidal frequencies is formulated first, followed by an introduction of different truncation methods and the minimum-norm solutions. Finally, comparisons of these three QR and the LS methods to the TSVD method are given based on computer simulations.

II. FBLP MODEL

Consider a complex-valued data sequence of length n ,

$$\bar{x}_i = \sum_{k=1}^p e^{j2\pi f_k i} + w_i \equiv x_i + w_i, \quad i = 1, 2, \dots, n \quad (1)$$

where p is the number of sinusoids and w_i is an additive white Gaussian noise with variance σ^2 . We define the signal-to-noise ratio (SNR) as $\text{SNR (dB)} = -10 \log(2\sigma^2)$ [3]. It can be shown [3], [1] that under noise-free conditions, the frequency locations can be obtained by finding the roots of

$$S(z) = 1 - \sum_{k=1}^l g_k z^{-k} = 0 \quad (2)$$

which are on the unit circle. The complex-valued coefficients g_k , $k = 1, 2, \dots, l$, satisfy the following system of FBLP equations:

$$\begin{bmatrix} x_l & x_{l-1} & \cdots & x_1 \\ x_{l+1} & x_l & \cdots & x_2 \\ \vdots & \vdots & \ddots & \vdots \\ x_{n-1} & x_{n-2} & \cdots & x_{n-l} \\ x_2^* & x_3^* & \cdots & x_{l+1}^* \\ x_3^* & x_4^* & \cdots & x_{l+2}^* \\ \vdots & \vdots & \ddots & \vdots \\ x_{n-l+1}^* & x_{n-l+2}^* & \cdots & x_n^* \end{bmatrix} \begin{bmatrix} g_1 \\ g_2 \\ \vdots \\ g_l \end{bmatrix} = \begin{bmatrix} x_{l+1} \\ x_{l+2} \\ \vdots \\ x_n \\ x_1^* \\ x_2^* \\ \vdots \\ x_{n-l}^* \end{bmatrix} \quad (3)$$

with l representing the order of the prediction model, and $*$ the complex conjugate. For simplicity, denote (3) as

$$Ag = b \quad (4)$$

where the data matrix A and the right-hand-side vector b are constructed from the data sequence $\{x_i | i = 1, \dots, n\}$ in a FBLP manner. We will assume that $p \leq l \leq n - p/2$ and $\text{rank}(A) = p$ [1, p. 343]. When the noise is present, we use an $\tilde{\cdot}$ on A and b , i.e., $\tilde{A} = A + E$ and $\tilde{b} = b + e$, to denote the noise-corrupted FBLP model with the additive noise. Equation (4) now becomes the FBLP LS problem of

$$\min_g \|\tilde{A}g - \tilde{b}\|_2 \quad (5)$$

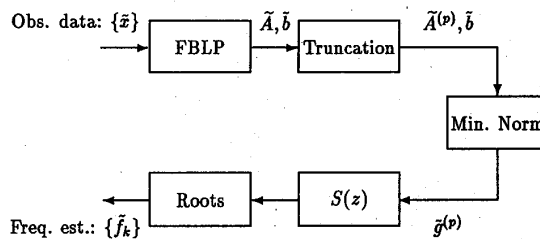


Fig. 1. Block diagram for sinusoidal frequency estimation based on the FBLP model.

where \tilde{A} has full rank due to the perturbation of the noise. One standard approach [3] is to use the TSVD method on (5) to obtain a rank- p approximation of the FBLP matrix \tilde{A} , denoted by $\tilde{A}_{\text{SVD}}^{(p)}$, followed by solving for a minimum norm LS solution of \tilde{g} given by

$$\tilde{A}_{\text{SVD}}^{(p)} \tilde{g} \equiv \tilde{b} \quad (6)$$

or equivalently, $\tilde{g} = [\tilde{A}_{\text{SVD}}^{(p)}]^\dagger \tilde{b}$, where $[\cdot]^\dagger$ denotes the pseudoinverse of a matrix. Then the frequencies can be computed by finding the phases of the roots of (2) close to the unit circle or searching for the peaks of $1/|S(\exp(j2\pi f))|^2$, $-0.5 \leq f < 0.5$. Notice that the proper choice of the prediction order l depends on p , the number of sinusoids, which may or may not be known in advance. Throughout our discussion, we will assume this quantity is known. If not, then the detection problem arises [2]. A detailed treatment of this problem involves various other basic issues and will not be addressed here. Fig. 1 depicts a flowchart diagram summarizing the estimation of harmonics frequencies based on the FBLP model.

III. TRUNCATION METHODS

In this section, we consider the rank- p approximation of the FBLP matrix \tilde{A} . We subsequently solve the corresponding system for the minimum-norm solution \tilde{g} . For many LS problems, ill-conditioning can be troublesome, and truncation methods are known to be useful in stabilizing the solutions at the cost of slightly increased residual errors [9]. Let

$$\tilde{A} = \tilde{U} \tilde{\Sigma} \tilde{V}^H = [\tilde{U}_1 \quad \tilde{U}_2] \begin{bmatrix} \tilde{\Sigma}_1 & 0 \\ 0 & \tilde{\Sigma}_2 \end{bmatrix} \begin{bmatrix} \tilde{V}_1^H \\ \tilde{V}_2^H \end{bmatrix} \quad (7)$$

$$\tilde{A} \Pi = \tilde{Q} \tilde{R} = [\tilde{Q}_1 \quad \tilde{Q}_2] \begin{bmatrix} \tilde{R}_{11} & \tilde{R}_{12} \\ 0 & \tilde{R}_{22} \end{bmatrix} \quad (8)$$

be the SVD and QRD of the $2(n-l) \times l$ complex-valued matrix \tilde{A} , respectively, where H denotes the complex-conjugate transpose of a complex-valued matrix or vector and Π is a column-permutation matrix and will be explained later. $\tilde{\Sigma}_1 = \text{diag}(\tilde{\sigma}_1, \dots, \tilde{\sigma}_p)$ and

$$\tilde{\Sigma}_2 = \begin{bmatrix} \text{diag}(\tilde{\sigma}_{p+1}, \dots, \tilde{\sigma}_l) \\ 0 \end{bmatrix}$$

represent nonincreasing singular values. $\tilde{R}_{11} \in \mathbb{C}^{p \times p}$, $\tilde{R}_{12} \in \mathbb{C}^{p \times (l-p)}$, and $\tilde{R}_{22} \in \mathbb{C}^{(l-p) \times (l-p)}$, while \tilde{R} is an upper-triangular matrix.

$$\tilde{U} = [\tilde{U}_1 \quad \tilde{U}_2] = [\tilde{u}_1, \dots, \tilde{u}_p, \tilde{u}_{p+1}, \dots, \tilde{u}_{2(n-l)}] \in \mathbb{C}^{2(n-l) \times 2(n-l)} \quad (9)$$

$$\tilde{V} = [\tilde{V}_1 \quad \tilde{V}_2] = [\tilde{v}_1, \dots, \tilde{v}_p, \tilde{v}_{p+1}, \dots, \tilde{v}_l] \in \mathbb{C}^{l \times l} \quad (10)$$

and

$$\tilde{Q} = [\tilde{Q}_1 \quad \tilde{Q}_2] = [\tilde{q}_1, \dots, \tilde{q}_p, \tilde{q}_{p+1}, \dots, \tilde{q}_l] \in \mathbb{C}^{2(n-l) \times l} \quad (11)$$

all have orthonormal columns, i.e., $\tilde{u}_i^H \tilde{u}_j = \tilde{v}_i^H \tilde{v}_j = \tilde{q}_i^H \tilde{q}_j = \delta_{ij}$.

In the absence of noise, $\tilde{\Sigma}_2 = \tilde{R}_{22} = 0$. Here the permutation matrix $\Pi = [\pi_1, \dots, \pi_l]$ is used to represent different methods of performing QRD with column interchanges. Now, we want to preserve as much of the energy as possible (with respect to the Frobenius norm defined below) in the trapezoidal matrix $[\tilde{R}_{11} \quad \tilde{R}_{12}]$ of (8). Equivalently, we want to leave as little energy as possible residing in the lower right submatrix \tilde{R}_{22} , which will be truncated. During the i th stage of the QRD procedure ($i = 1, \dots, l$), the submatrix \tilde{R}_{22} has $l - i + 1$ columns. In the dynamic column-swapping case the column of \tilde{R}_{22} having the largest 2-norm is permuted into the first column position [9]. This is the column with the maximum linear independence with the subspace defined by $[\tilde{q}_1, \dots, \tilde{q}_{i-1}]$. This process forces the energy in the remaining portion of \tilde{R}_{22} to be as small as possible. Hence, the subsequent truncation of \tilde{R}_{22} results in the smallest possible error.

There are at least three possible methods for determining the permutation matrix Π while performing QRD. They are:

1) For QRD with no pivoting, Π is simply an identity matrix. We denote this scheme as the TQR method.

2) QRD with preordered columns [6] determines Π according to a column index maximum-difference bisection rule. Here we select the first and the l th columns, followed by the column $\lceil (1+l)/2 \rceil$ halfway between 1 and l . Then we pick the columns that lie in the midway of those ones previously selected, i.e., $\lceil (1 + \lceil (1+l)/2 \rceil)/2 \rceil$, $\lceil (\lceil (1+l)/2 \rceil + l)/2 \rceil$, and so on. This selection rule does not depend on the real-time data in \tilde{A} . The underlying reason for this ad hoc fixed-ordering scheme is to provide the selected columns with a possibly maximum differences or minimum linear dependency among these columns. This ordering scheme is not unique nor is optimum in general. It was motivated due to the nature of the matrix \tilde{A} arranged in the form of (3) consisting of perturbed sums of harmonic sinusoids. As an example, suppose there are 5 columns, then the preordering strategy leads to [1]-[5]. Thus we have $\Pi = [e_1, e_5, e_3, e_2, e_4]$, where e_i is a dimension l column vector with all zero components except for an one at the i th position. We denote this scheme as the TQRR method. It applies only when the frequencies of the input signal components are closely spaced.

3) As for QRD with column pivoting [9, p. 233], Π is determined during the QRD process, where $\pi_i = e_{d_i}$ and $d_i \in [1, l]$ is the index such that \tilde{a}_{d_i} , the d_i th column of \tilde{A} , has the largest norm. Continuing with this column-pivoting process on the lower right submatrix yet to be triangularized, we can determine the permutation matrix Π which yields an optimum QRD column ordering strategy in the sense of preserving most energy in the upper trapezoidal submatrix. However, this Π is data-dependent and the extra cost for this pivoting may make it less desirable for some applications. We denote this scheme as the TQRP method.

After forcing those weak-rank quantities to be zero and preserving the most significant p -rank, we can obtain a rank- p approximate of \tilde{A} . These weak-rank quantities are those entries in the factorized matrix that contribute least significantly to the matrix, or possess the smallest portion of the energy (square of Frobenius norm) of

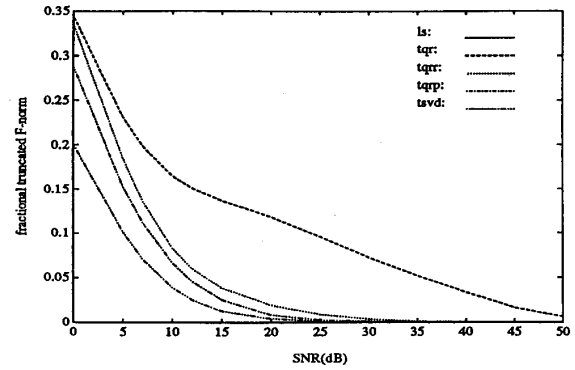


Fig. 2. Average fractional truncated Frobenius norms.

the associated matrix. For TSVD, $\tilde{\Sigma}_2$ is discarded and

$$\tilde{A}_{\text{TSVD}}^{(p)} = \tilde{U}_1 \tilde{\Sigma}_1 \tilde{V}_1^H. \quad (12)$$

Similarly, for TQR, the lower right submatrix \tilde{R}_{22} is discarded and

$$\tilde{A}_{\text{TQR}}^{(p)} \Pi = \tilde{Q}_1 [\tilde{R}_{11} \quad \tilde{R}_{12}]. \quad (13)$$

To account for the effect due to truncation, we define the fractional truncated F-norm as

$$\mathfrak{F}^{(p)} = 1 - \|\tilde{A}^{(p)}\|_F / \|\tilde{A}\|_F \quad (14)$$

where $\|\cdot\|_F$ is the Frobenius norm given by

$$\|A\|_F = \sqrt{\sum_i \sum_j |a_{ij}|^2} = \sqrt{\text{tr}(A^H A)}. \quad (15)$$

Thus we have

$$\mathfrak{F}_{\text{TSVD}}^{(p)} = \sqrt{\frac{\sum_{j=p+1}^l \tilde{\sigma}_j^2}{\sum_{j=1}^l \tilde{\sigma}_j^2}} \quad (16)$$

and

$$\mathfrak{F}_{\text{TQR}}^{(p)} = 1 - \left(\frac{\|\tilde{R}_{11}\|_F^2 + \|\tilde{R}_{12}\|_F^2}{\|\tilde{R}_{11}\|_F^2 + \|\tilde{R}_{12}\|_F^2 + \|\tilde{R}_{22}\|_F^2} \right)^{1/2}. \quad (17)$$

While

$$0 \leq \mathfrak{F}_{\text{TSVD}}^{(p)} \leq \mathfrak{F}_{\text{TQRP}}^{(p)} \leq 1 \quad (18)$$

is valid analytically [9], from extensive computations we also observed the relationships among truncated QR methods to satisfy

$$\mathfrak{F}_{\text{TQRP}}^{(p)} \leq \mathfrak{F}_{\text{TQRR}}^{(p)} \leq \mathfrak{F}_{\text{TQR}}^{(p)} \leq 1. \quad (19)$$

Therefore, from the point of view of preserving the Frobenius norm (square root of energy) of a matrix, SVD provides the optimum truncation, with TQRP being next, while TQRR and TQR truncate even more (see Fig. 2).

IV. MINIMUM-NORM SOLUTIONS

After truncation, the FBLP LS problem becomes rank-deficient, hence the minimum-norm LS solution is desired in order to suppress those spurious harmonics in the pseudo-spectrum. For TSVD it is given by

$$\tilde{g}_{\text{TSVD}}^{(p)} = \tilde{V}_1 \tilde{\Sigma}_1^{-1} \tilde{U}_1^H \tilde{b}. \quad (20)$$

After the QRD and truncation of \tilde{R}_{22} , the FBLP system assumes the following form:

$$[\tilde{R}_{11} \ \tilde{R}_{12}]g = \tilde{Q}_1 b \quad (21)$$

where the matrix on the left is of dimension $p \times l$, $l > p$. We therefore observe the original overdetermined FBLP system of equations given by (3) converted into an underdetermined system. To obtain $\tilde{g}_{\text{TQR}}^{(p)}$ corresponding to (21), we can perform a QRD on the right of the trapezoidal upper triangular matrix in (13) to zero out \tilde{R}_{12} and also obtain the orthonormal row space, \tilde{T}^H , of $[\tilde{R}_{11} \ \tilde{R}_{12}]$. That is

$$\tilde{A}_{\text{TQR}}^{(p)} \Pi = \tilde{Q}_1 [\tilde{R}_{11} \ \tilde{R}_{12}] = \tilde{Q}_1 \tilde{L}^H \tilde{T}^H \quad (22)$$

where $\tilde{T} = [\tilde{t}_1, \dots, \tilde{t}_p] \in \mathcal{C}^{l \times p}$ has orthonormal columns and $\tilde{L}^H \in \mathcal{C}^{p \times p}$ is an upper triangular matrix. This is sometimes called a complete orthogonal factorization [9, p. 236], and we can consider it as a two-sided direct unitary transformation on a rank-deficient matrix to compress all the energy of a matrix into a square upper triangular matrix. Then from (22) the minimum-norm solution for the underdetermined LS problem

$$\tilde{A}_{\text{TQR}}^{(p)} \tilde{g} = \tilde{b} \quad (23)$$

follows by

$$\begin{aligned} \tilde{g}_{\text{TQR}}^{(p)} &= \Pi \begin{bmatrix} \tilde{R}_{11}^H \\ \tilde{R}_{12}^H \end{bmatrix} (\tilde{R}_{11} \tilde{R}_{11}^H + \tilde{R}_{12} \tilde{R}_{12}^H)^{-1} \tilde{Q}_1^H \tilde{b} \\ &= \Pi \tilde{T} \tilde{L}^{-H} \tilde{Q}_1^H \tilde{b}. \end{aligned} \quad (24)$$

In summary, $\tilde{g}_{\text{TQR}}^{(p)}$ in (24) for various TQR methods can be obtained in a backward manner. We first perform the QRD and also determine the permutation matrix Π and the transformed right-hand-side vector $\tilde{Q}_1^H \tilde{b}$ as given in (13). After performing another QRD on the truncated upper triangular matrix in (22) we can obtain \tilde{T} and \tilde{L} . Next, a back substitution for $\tilde{L}^{-H} \tilde{Q}_1^H \tilde{b}$ followed by a matrix-vector multiplication and a vector permutation results in $\tilde{g}_{\text{TQR}}^{(p)}$.

V. SIMULATION RESULTS

Finally, we present various computer simulations based on the following model. Let $\tilde{x}_i = \cos(2\pi f_1 i) + \cos(2\pi f_2 i) + w_i$, $i = 1, 2, \dots, 48$, with $f_1 = 0.125$, $f_2 = 0.135$, $l = 36$ and $\{w_i\}$ is a white Gaussian random sequence. The estimated frequencies, \hat{f}_1 and \hat{f}_2 , are determined by the phase (from 0 to π) of complex roots closest to the unit circle. For TQRR, we prepermute the columns of the FBLP matrix in the order of: $\{1 \ 36 \ 18 \ 9 \ 27 \ 5 \ \dots\}$ as suggested by [6]. We will consider the frequency bias and the standard deviation of the estimated frequency on the evaluation of the performances. Two classes of comparisons will be considered in the following curves. The first one is to compare these truncation methods under various values of SNR from 0 to 50 dB. The second is to observe the asymptotic performance by fixing the order $l = 36$, and increasing the number of observed data samples. One hundred independent simulations are used to obtain the statistical means and standard deviations.

Fig. 2 gives the average fractional truncated Frobenius norms of (15) versus SNR when we preserve only the four most significant ranks of the FBLP matrix for the five different methods. This confirms their relationships in (18) and (19) and also shows that the truncated energy decreases monotonically as SNR increases. We note that the solid curve for the LS case coincides with the SNR axis due to no truncation at all. Fig. 3 shows the standard deviation of \hat{f}_2 . We can see the TQRP competes quite well with TSVD, while TQRR performs slightly worse than TQRP but better than TQR without pivoting.

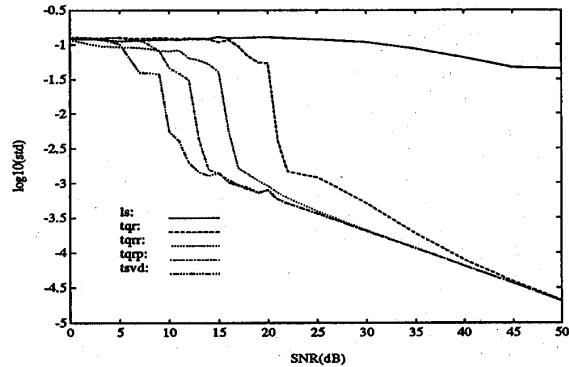


Fig. 3. Standard deviations for estimating $f_2 = 0.135$ using a 24×36 FBLP matrix.

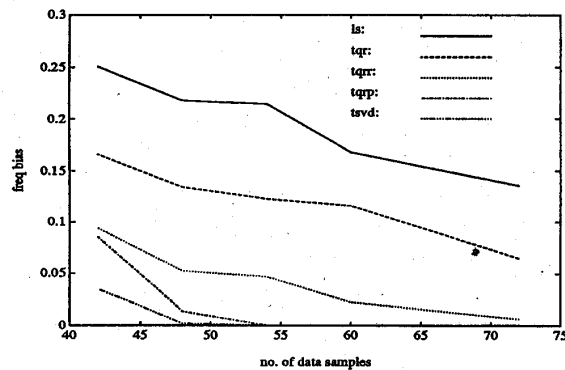


Fig. 4. Mean frequency bias versus the number of data samples for $f = \{0.125, 0.135\}$, SNR = 10 dB, and order = 36.

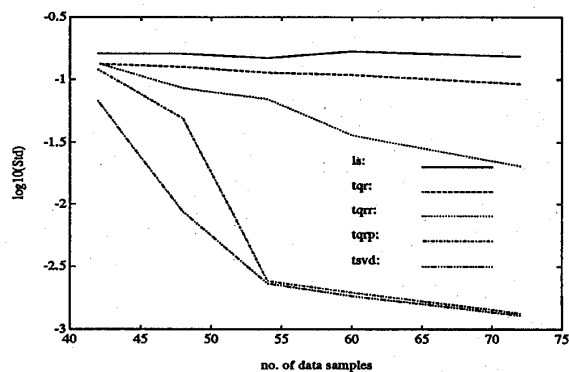


Fig. 5. Standard deviations of estimates versus the number of data samples for $f = \{0.125, 0.135\}$, SNR = 10 dB, and order = 36.

If we fix the SNR = 10 dB and the order of the FBLP model to be $l = 36$, as more data are collected, the ill effects of the noise should be asymptotically smoothed out. Fig. 4 shows the combined average frequency bias (defined as the sum of the absolute values of the biases for f_1 and f_2) versus the number of data samples. Fig. 5 shows the curves of various combined standard deviations of the estimated frequencies which is defined as the square root of the sum of squares of the standard deviations of each frequency estimate. From Figs. 4 and 5, it is clear that under moderate SNR conditions,

TABLE I
COMPARISONS OF TRUNCATED LEAST SQUARES METHODS

	Freq. Est.	Comput. Cost	VLSI	Updating
TSVD	Excellent	Very high	Complex	Difficult
TQRP	Very good	Medium	Medium	Medium
TQRR	Good	Fair	Fair	Easy
TQR	Fair	Fair	Fair	Easy
LS	Poor	Low	Low	Easy

the performances of TQRP closely follow that of TSVD. Throughout our simulation, we have fixed the model order $l = 36$. This choice is optimal for the TSVD method. As for the proposed three TQR methods, further investigation and extensive simulations need to be performed to see its effects.

VI. CONCLUSIONS

Three truncated QR methods have been proposed for resolving closely spaced frequencies. Well known for their numerical stability and ease in updating, these TQR methods, at the cost of slightly degraded performance, are promising for real-time applications. Table I summarizes the comparisons among different truncation methods. From our simulations, we found that the ratio of flops counts of SVD, QR with reordering, QR with column pivoting, and standard QRD is about 5.9:1.1:1.1:1. This comparison is based on factorization of a 24×36 matrix using PC-MATLAB. We conclude that TQR is the simplest and can be performed easily in a real time updating, but may suffer significant degradation. TQRP provides almost the same performance as SVD, but is not easy to implement in real time processing in that the difficult column reshuffling is required while performing QRD with pivoting. TQRR provides a good compromise between the above two and can also be implemented for systolic array processing. The LS method is simple to implement and update but has a poor frequency estimation capability.

ACKNOWLEDGMENT

The authors would like to thank the reviewers for their valuable comments and suggestions.

REFERENCES

- [1] S. Haykin, *Adaptive Filter Theory*. Englewood Cliffs, NJ: Prentice-Hall, 1986.
- [2] S. M. Kay, *Modern Spectral Estimation: Theory and Application*. Englewood Cliffs, NJ: Prentice-Hall, 1988.
- [3] D. W. Tufts and R. Kumaresan, "Estimation of frequencies of multiple sinusoids: Making linear prediction perform like maximum likelihood," *Proc. IEEE*, vol. 70, no. 9, pp. 975-989, Sept. 1982.
- [4] M. Kaveh and A. J. Barabell, "The statistical performance of MUSIC and the minimum norm algorithms in resolving plane waves in noise," *IEEE Trans. Acoust., Speech, Signal Processing*, vol. ASSP-34, no. 2, pp. 331-340, Apr. 1986.
- [5] B. D. Rao, "Perturbation analysis of an SVD-based linear prediction method for estimating the frequencies of multiple sinusoids," *IEEE Trans. Acoust., Speech, Signal Processing*, vol. 36, no. 7, pp. 1026-1035, July 1988.
- [6] J. P. Reilly, W. G. Chen, and K. M. Wong, "A fast QR-based array-processing algorithm," *Proc. SPIE Int. Soc. Opt. Eng.*, pp. 36-47, 1988.
- [7] S. L. Marple, Jr., "A tutorial overview of modern spectral estimation," in *Proc. IEEE ICASSP*, 1989, pp. 2152-2157.
- [8] W. M. Gentleman and H. T. Kung, "Matrix triangularization by systolic array," in *Proc. SPIE Int. Soc. Opt. Eng.*, vol. 298, pp. 19-26, 1981.
- [9] G. H. Golub and C. F. Van Loan, *Matrix Computations*, 2nd ed. Baltimore, MD: Johns Hopkins University Press, 1989.
- [10] J. R. Bunch and C. P. Nielsen, "Updating the singular value decomposition," *Numer. Math.*, vol. 31, pp. 111-129, 1978.
- [11] P. Comon and G. H. Golub, "Tracking a few extreme singular values and vectors in signal processing," *Proc. IEEE*, vol. 78, no. 8, pp. 1327-1343, Aug. 1990.

The Double Bilinear Transformation for 2-D Systems in State-Space Description

P. Agathoklis

Abstract—The double bilinear transformation for two-dimensional (2-D) systems described by state-space models is considered. The relationships between the realization matrices of the continuous and the discrete 2-D transfer functions are presented.

I. INTRODUCTION

The bilinear transformation has been widely used to transform continuous prototypes into discrete transfer functions. For one-dimensional (1-D) systems it has been studied for systems described by transfer functions, as well as by state-space models [1], and has been used in many filter design techniques and control design applications. In the two-dimensional (2-D) case, the double bilinear transformation has been used to design 2-D digital filters ([4], [5] are examples of such techniques), as well as for double integral evaluations [2] of systems described by transfer functions.

In this correspondence, the double bilinear transformation for 2-D systems described by state-space models is considered. The relationships between the realization matrices of the discrete and the continuous transfer functions are given.

II. PRELIMINARIES

Consider a 2-D discrete system represented by a 2-D state-space model [3]:

$$\begin{bmatrix} x^h(i+1, j) \\ x^v(i, j+1) \end{bmatrix} = \begin{bmatrix} A_{11d} & A_{12d} \\ A_{21d} & A_{22d} \end{bmatrix} \begin{bmatrix} x^h(i, j) \\ x^v(i, j) \end{bmatrix} + \begin{bmatrix} B_{1d} \\ B_{2d} \end{bmatrix} u(i, j) \quad (1a)$$

$$y(i, j) = [C_{1d} \quad C_{2d}] \begin{bmatrix} x^h(i, j) \\ x^v(i, j) \end{bmatrix} + D_c u(i, j) \quad (1b)$$

where $x^h \in R^n$ and $x^v \in R^m$ represent the horizontal and vertical states respectively, u is the input and y the output. The system transfer matrix is given by

$$H(z_1, z_2) = D_d + [C_{1d} \quad C_{2d}] [Z - A_d]^{-1} \begin{bmatrix} B_{1d} \\ B_{2d} \end{bmatrix} \quad (2)$$

Manuscript received March 12, 1992; revised June 6, 1992. This work was supported by the NSERC.

The author is with the Department of Electrical and Computer Engineering, University of Victoria, Victoria, B. C., V8W 3P6, Canada. IEEE Log Number 9205119.